CHEMISTRY
A EUROPEAN JOURNAL

An EPR and ENDOR Investigation of a Series of Diazabutadiene–Group 13 Complexes

Robert J. Baker, Robert D. Farley, Cameron Jones,* David P. Mills, Marc Kloth, and Damien M. Murphy*[a]

Abstract: Paramagnetic diazabutadienegallium(II or III) complexes, [(Ar-DAB)$_2$Ga] and [{(Ar-DAB$^{\bullet}$)GaX}$_2$] (X = Br or I; Ar-DAB = {N(Ar)C(H)}$_2$, Ar = 2,6-diisopropylphenyl), have been prepared by reactions of an anionic gallium N-heterocyclic carbene analogue, [K(tmeda)][:Ga(Ar-DAB)], with either "GaI" or [$MoBr_2(CO)_2(PPh_3)_2$]. A related In^{III} complex, [(Ar-DAB$^{\bullet}$)$InCl_2$(thf)], has also been prepared. These compounds were characterised by X-ray crystallography and EPR/ENDOR spectroscopy. The EPR spectra of all metal(III) complexes incorporating the Ar-DAB ligand, [(Ar-DAB$^{\bullet}$)$MX_2(thf)_n$] (M = Al, Ga or In; X = Cl or I; n = 0 or 1) and [(Ar-DAB)$_2$Ga], confirmed that the unpaired spin density is primarily ligand centred, with weak hyperfine couplings to Al (a = 2.85 G), Ga (a = 17—25 G) or In (a = 26.1 G) nuclei. Changing the N substituents of the diazabutadiene ligand to *tert*-butyl groups in the gallium complex, [(*t*Bu-DAB$^{\bullet}$)GaI_2] (*t*Bu-DAB = {N(*t*Bu)C(H)}$_2$), changes the unpaired electron spin distribution producing ^{1}H and ^{14}N couplings of 1.4 G and 8.62 G, while the aryl-substituted complex, [(Ar-DAB$^{\bullet}$)GaI_2], produces couplings of about 5.0 G. These variations were also manifested in the gallium couplings, namely a_{Ga} ~1.4 G for [(*t*Bu-DAB$^{\bullet}$)GaI_2] and a_{Ga} ~25 G for [(Ar-DAB$^{\bullet}$)GaI_2]. The EPR spectra of the gallium(II) and indium(II) diradical complexes, [{(Ar-DAB$^{\bullet}$)GaBr}$_2$], [{(Ar-DAB$^{\bullet}$)GaI}$_2$], [{(*t*Bu-DAB$^{\bullet}$)GaI}$_2$] and [{(Ar-DAB$^{\bullet}$)InCl}$_2$], revealed doublet ground states, indicating that the Ga–Ga and In–In bonds prevent dipole–dipole coupling of the two unpaired electrons. The EPR spectrum of the previously reported complex, [(Ar-BIAN$^{\bullet}$)GaI_2] (Ar-BIAN = bis(2,6-diisopropylphenylimino)acenaphthene) is also described. The hyperfine tensors for the imine protons, and the aryl and *tert*-butyl protons were obtained by ENDOR spectroscopy. In [(Ar-DAB$^{\bullet}$)-GaI_2], gallium hyperfine and quadrupolar couplings were detected for the first time.

Keywords: ENDOR spectroscopy · EPR spectroscopy · gallium · Group 13 elements · radicals · structure elucidation

Introduction

Paramagnetic heavier main group element compounds having an unpaired electron primarily located on the heavy element centre have generated considerable interest.[1] In contrast to the large number of known Group 14 element centred radicals, there are fewer examples of complexes exhibiting aluminium-, gallium- or indium-centred radicals. The majority of the stable radical species of these elements have the spin delocalised over unsaturated organic substituents. Some examples include [*i*Bu$_2$Al(2,2′-bipyridyl)],[2] [M(dpt)$_3$] (M = Al, Ga or In; dpt = tris-1,3-diphenyltriazenido)[3] or [(*t*Bu-DAB)$_2$M] (M = Al[4] or Ga;[5] *t*Bu-DAB = {N(*t*Bu)C(H)}$_2$). The gallium complex of the *t*Bu-DAB ligand was initially interpreted as possessing gallium in the +2 oxidation state on the basis of a dominant ^{69,71}Ga-radical coupling observed by EPR spectroscopy. A later report on this complex described it as a Ga^{III} complex containing one doubly reduced and one singly reduced *t*Bu-DAB ligand.[6] This view was supported by extended Hückel calculations which predicted two degenerate HOMOs having very little gallium contribution.[7] It is worthy of note that a range of other paramagnetic complexes incorporating the *t*Bu-DAB ligand and various metals, for example, Li,[8] Mg[9] and Zn,[8] have been prepared and studied by EPR spectroscopy and X-ray crystallography.

[a] Dr. R. J. Baker, Dr. R. D. Farley, Prof. C. Jones, D. P. Mills, Dr. M. Kloth, Dr. D. M. Murphy
School of Chemistry, Cardiff University
PO Box 912, Cardiff CF10 3AT (UK)
Fax: (+44) 2920-874-030
E-mail: jonesca6@cardiff.ac.uk
murphydm@cardiff.ac.uk

Supporting information for this article is available on the WWW under http://www.chemeurj.org/ or from the author.

DOI: 10.1002/chem.200401103

Our interest in diazabutadiene complexes of Group 13 metals arose from the reaction of the Ar-DAB ligand (Ar-DAB = {N(Ar)C(H)}$_2$, Ar = 2,6-diisopropylphenyl) with In^{I}Cl. The product from this reaction was the unusual In^{II} diradical dimeric complex, [{(Ar-DAB$^{\bullet}$)InCl}$_2$].[10] This work was expanded to a study of the reactivity of both *t*Bu-DAB and Ar-DAB toward "GaI" which led to the isolation of the Ga^{II} dimer, [{(*t*Bu-DAB$^{\bullet}$)GaI}$_2$], and the monomeric Ga^{III} complexes, [(Ar-DAB$^{\bullet}$)GaI$_2$] and [(*t*Bu-DAB$^{\bullet}$)GaI$_2$], each featuring singly reduced diazabutadiene ligands.[11] It is noteworthy that one of these complexes, [(Ar-DAB$^{\bullet}$)GaI$_2$], was independently reported by another group at about the same time.[12] Other Group 13-diazabutadiene complexes we have studied include [(Ar-DAB$^{\bullet}$)AlI$_2$],[11] [(*t*Bu-DAB$^{\bullet}$)Ga{E(SiMe$_3$)$_2$}$_n$I$_{2-n}$] (E = N, P or As; n = 1 or 2)[13] and [(Ar-BIAN$^{\bullet}$)-GaI$_2$] (Ar-BIAN = bis(2,6-diisopropylphenylimino)-acenaphthene).[14]

Subsequently, we showed that the reduction of [(Ar-DAB$^{\bullet}$)-GaI$_2$] with potassium metal leads to the isolation of a novel anionic Ga^{I} heterocycle, [:Ga(Ar-DAB)]$^-$,[11] which is a valence-isoelectronic analogue of N-heterocyclic carbenes and is closely related to the anion, [:Ga(*t*Bu-DAB)]$^-$ reported by Schmidbaur et al.[15] Given the importance of the N-heterocyclic carbenes as ligands, we have initiated an investigation of the reactivity of [:Ga(Ar-DAB)]$^-$ towards main group[16] and transition-metal precursors.[17] Herein, we detail the preparation and characterisation of several paramagnetic complexes derived from that investigation. These complexes, and several previously reported species, have been examined by continuous wave electron paramagnetic resonance (EPR) and electron nuclear double resonance (ENDOR) spectroscopies. While EPR provides information on the localised spin distribution, through the hyperfine couplings, the weaker interactions between the unpaired electron and the remote magnetic nuclei of the ligand can be detected by ENDOR spectroscopy. In this way we have obtained a detailed view on the extent of spin delocalisation in the complexes, and how this spin distribution is influenced by the substituents on the diazabutadiene ligand.

Results and Discussion

The compounds **1**–**10** discussed in this paper are shown in Scheme 1. The syntheses and structures of complexes **4**, **5**, **6** and **8** have not been previously reported. In the case of **4**–**6**, these have been synthesised by the reactions of the Ga^{I} N-heterocyclic carbene analogue [K(tmeda)][:Ga(Ar-DAB)] (tmeda = tetramethylethylenediamine)with transition-metal and main group metal precursors. The reaction of this heterocycle with "GaI" gave two products, **4** and **6**, in low yield. The mechanism of this reaction is at present unknown but seemingly involves a series of disproportionation and ligand rearrangement reactions, as evidenced by the precipitation of gallium metal. It is worthy of note that the reduced, diamagnetic anionic analogue of **4**, namely [K(dme)$_4$][Ga(Ar-DAB)$_2$] (dme = dimethoxyethane), has been reported.[16] Complex **5** resulted from the 1:1 reaction of the gallium carbene analogue with [MoBr$_2$(CO)$_2$(PPh$_3$)$_2$]. The formation of **5** probably involves an initial oxidative insertion of the Ga^{I} centre into the Mo–Br bond of the molybdenum complex. Homolytic cleavage of the resultant Ga–Mo bond and dimerisation of the generated gallium radical could then lead to **5**. Related insertions of Group 13 metal(I) alkyls into transition-metal halide bonds have been reported.[18] Complex **8** was prepared in low yield by the reaction of [(Ar-DAB)Li$_2$] (generated in situ by the reaction of Ar-DAB and Li powder) with InCl in THF. The only other products that could be isolated from this reaction were Ar-DAB and indium metal, again suggesting a disproportionation mechanism is involved in the formation of **8**.

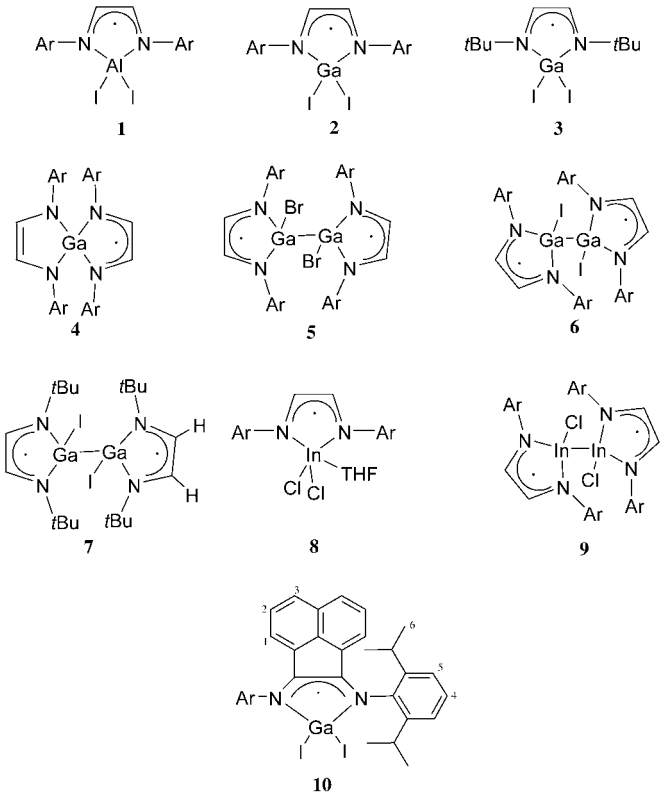

Scheme 1. Compounds investigated in this study.

The identities of complexes **4**, **5**, **6** and **8** have been confirmed by X-ray crystallography and their molecular structures are shown in Figure 1, Figure 2, Figure 3, Figure 4, respectively. The bond lengths within the two diazabutadiene frameworks for **4** are different, indicating that one ligand has been doubly reduced whilst the other is singly reduced and has an unpaired electron delocalised over the ligand. This is a very similar situation to that seen for [(*t*Bu-DAB)$_2$Ga].[5–7] Compounds **5** and **6** are isostructural, centrosymmetric dimers in which the Ga^{II} centres sit in distorted tetrahedral environments. The metrical parameters for the complexes suggest a degree of delocalisation over the diazabutadiene ligands and their geometries are very close to that previously reported for the related complex, [{(*t*Bu-

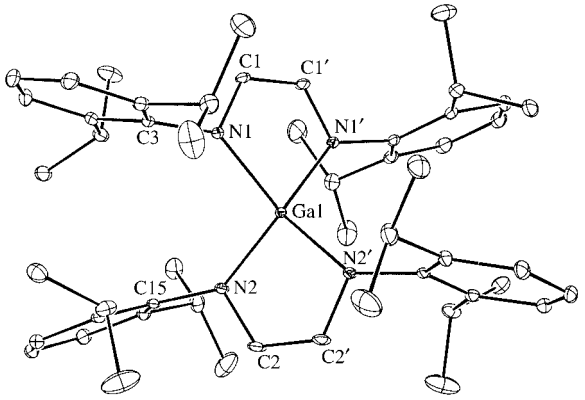

Figure 1. Molecular structure of **4**. Selected bond lengths [Å] and angles [°]: Ga1–N1 2.0073(17), Ga1–N2 1.9013(18), N1–C1 1.332(3), N2–C2 1.392(3), C1–C1′ 1.387(4), C2–C2′ 1.338(5); N1-Ga1-N1′ 82.07(10), N1-Ga1-N2 104.83(8), N1-Ga1-N2′ 145.71(8), N2-Ga1-N2′ 88.33(11). Symmetry transformation used to generate equivalent atoms ′: $-x$, y, $-z+1/2$.

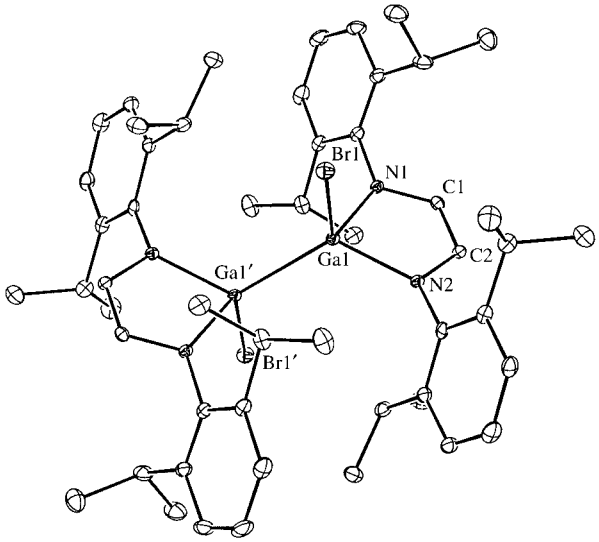

Figure 2. Molecular structure of **5**. Selected bond lengths [Å] and angles [°]: Ga1–Ga1′ 2.4662(12), Ga1–N1 1.983(3), Ga1–N2 1.981(3), Ga1–Br1 2.3738(7), N1–C1 1.346(4), N2–C2 1.340(4), C1–C2 1.384(5); N1-Ga1-N2 83.91(11), N1-Ga1-Br1 104.25(9), N1-Ga1-Ga1′ 123.39(9), N2-Ga1-Br1 104.44(8), N2-Ga1-Ga1′ 122.89(9), Br1-Ga1-Ga1′ 113.22(3). Symmetry transformation used to generate equivalent atoms ′: $-x+2$, $-y+1$, $-z+1$.

DAB^{-})GaI$\}_2$].[11] The structure of complex **8** shows it to be monomeric with a distorted trigonal bipyramidal indium centre having N1, Cl1 and Cl2 in equatorial sites. It is interesting that this complex includes a THF molecule of coordination, whereas the gallium analogue, **2**, is four-coordinate.[11,12] This difference most likely results from the larger covalent radius of indium relative to gallium. Again, the bond lengths within the diazabutadiene backbone are strongly suggestive of delocalisation over that ligand. The In–N bond lengths of 2.19 Å (av) in **8** are shorter than those seen for the neutral, diamagnetic complex, [InBr$_3$(Ar-DAB)] (2.32 Å av),[19] but similar to those in **9** (2.16 Å av).[10]

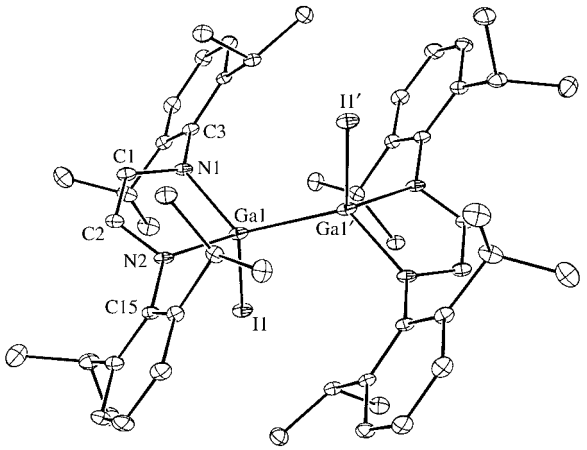

Figure 3. Molecular structure of **6**. Selected bond lengths [Å] and angles [°]: Ga1–Ga1′ 2.5755(16), Ga1–N1 1.984, Ga1–N2 1.997(4), Ga1–I1 2.5855(8), N1–C1 1.339(7), N2–C2 1.332(6), C1–C2 1.411(6); N1-Ga1-N2 83.95(16), N1-Ga1-I1 106.17(12), N1-Ga1-Ga1′ 121.84(13), N2-Ga1-I1 104.85(12), N2-Ga1-Ga1′ 121.78(12), I1-Ga1-Ga1′ 113.75(4). Symmetry transformation used to generate equivalent atoms ′: $-x$, $-y+1$, $-z$.

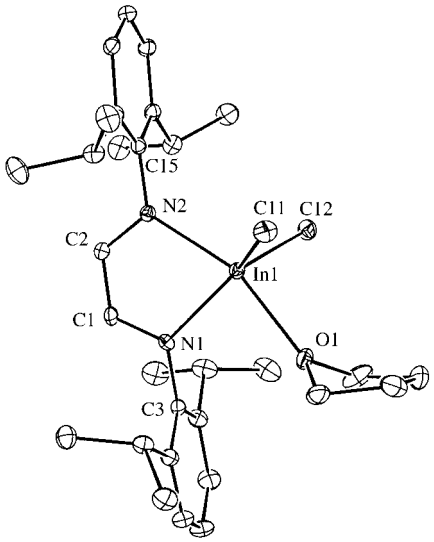

Figure 4. Molecular structure of **8**. Selected bond lengths [Å] and angles [°]: In1–N1 2.157(4), In1–N2 2.230(4), In1–O1 2.290(4), In1–Cl1 2.3646(15), In1–Cl2 2.3627(17), N1–C1 1.341(7), C1–C2 1.384(8), N2–C2 1.321(7), N1-In1-N2 77.01(16), N1-In1-O1 83.41(16), N1-In1-Cl1 127.39(12), N1-In1-Cl2 120.68(12), N2-In1-O1 160.25(15), N2-In1-Cl1 99.78(12), N2-In1-Cl2 101.47(12), Cl1-In1-Cl2 111.50(6), Cl1-In1-O1 88.98(12), Cl2-In1-O1 90.67(11).

EPR investigations: Owing to the paramagnetic nature of complexes **1**–**10**, EPR spectroscopy was used to determine the electronic structure and unpaired spin density in all cases. The EPR spectra were recorded at room temperature in isotropic fluid solutions, providing high resolution measurements of the isotropic hyperfine coupling constants. Owing to the small g and A anisotropy, and the substantial delocalisation of the unpaired electron in the π-based organic radicals of **1**–**10**, their low-temperature EPR spectra were virtually unresolved and did not provide any additional in-

formation. In these cases, continuous wave (cw) ENDOR was used to investigate the long-range weak hyperfine interactions to obtain a complete picture of the extent of electron delocalisation in the ligands involved. The ENDOR results will be discussed in the next section. While the EPR spectra for some of these complexes (**1**, **2**, **3**, **7** and **9**) have been previously reported by us and others,[10–12] none of the associated ENDOR spectra have been described.

The isotropic EPR spectra of **4** and **6** are shown in Figure 5 and Figure 6 respectively. The high resolution of the spectra facilitated their simulations and the extraction of

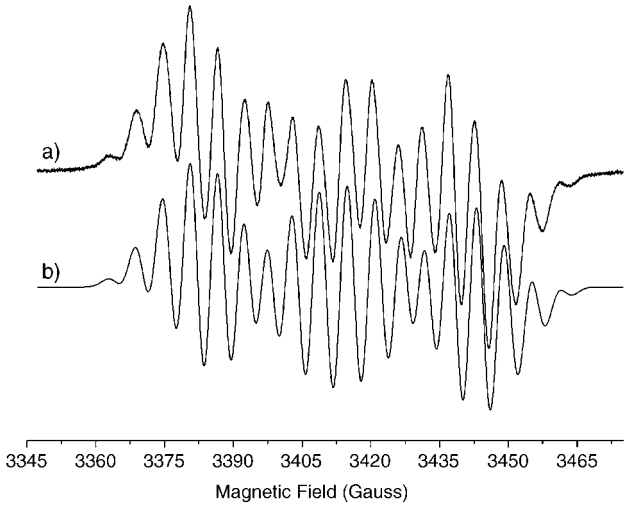

Figure 5. X-band EPR spectrum of **4** recorded at 298 K in 1:1 CD_2Cl_2/$C_6D_5CD_3$. a) experimental, b) simulated.

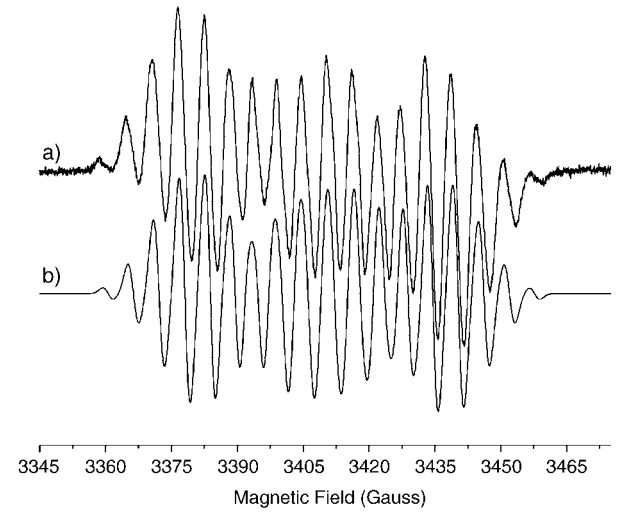

Figure 6. X-band EPR spectrum of **6** recorded at 298 K in 1:1 CD_2Cl_2/$C_6D_5CD_3$. a) experimental, b) simulated.

the hyperfine couplings (HFC). In particular, unambiguous identification of the separate HFC's, with different relative intensities, due to the two gallium isotopes (^{69}Ga: $I=3/2$, $a_o=4356$ G, 60.1% natural abundance; ^{71}Ga: $I=3/2$, $a_o=5535$G, 39.9% natural abundance) was possible. This confirmed that the magnitude of the isotropic HFC to ^{69}Ga and ^{71}Ga was $a_{Ga}=17.0$G and $a_{Ga}=20.5$ G, respectively, in both the monomeric, **4**, and dimeric, **6**, complexes. In addition, the ^{1}H and ^{14}N couplings were found to be $a_H=5.8$ G and $a_N=6.0$ G, respectively, in both complexes. The EPR spectra in Figure 5 and Figure 6 can therefore be explained as originating from the superimposition of overlapping triplets (due to two equivalent protons), quintets (due to two equivalent nitrogen atoms) and quartets (due to one gallium nucleus). The resulting HFC values for these complexes are presented in Table 1.

Hyperfine couplings to four magnetically equivalent nitrogen nuclei were reported for the [(*t*Bu-DAB)$_2$Ga] monoanion radical,[5–7] suggesting a dynamic Jahn–Teller distortion in the gallium complex with the unpaired electron "jumping" between the ligands on the EPR time scale. However, the EPR simulation of our closely related [(Ar-DAB)$_2$Ga] complex, **4**, clearly revealed that the unpaired electron interacts with only two magnetically equivalent nitrogen atoms, and is therefore located on one of the two Ar-DAB ligands.

These HFCs observed for **4** and **6** are in good agreement with our previous work which highlighted the important role played by bulky groups (i.e., *t*butyl or aryl) at the 1,4 positions of the diazabutadiene ligand (see Scheme 1) in modulating the extent of unpaired electron delocalisation in these paramagnetic complexes.[10,11] For example, for complexes with *tert*-butyl groups in the 1,4 positions, the ^{1}H and ^{14}N couplings were systematically found to be $a_H \approx 1.4$ G and $a_N \approx 8.6$ G (e.g., in the monomeric, **3**, and dimeric, **7**, complexes). However, in complexes with Ar groups at the 1,4 positions of the diazabutadiene ligand, the ^{1}H and ^{14}N couplings were found to be $a_H \approx 5.8$ G and $a_N \approx 6.0$ G, respectively (e.g., in complexes **4** and **6**). Clearly, the presence of these electron-withdrawing or -donating groups significantly influences the unpaired spin distributions within the diazabutadiene ligand. Despite this effect, it is clear that the spin density is primarily ligand centred (ca. >99%) in all complexes as expected based on a recent discussion of the electronic structure and bonding of main group diazabutadiene complexes with B, Al, Ga and In, where no sizable contribution of spin density was predicted at the central atom.[20] This agrees with our findings where the observed HFCs, and therefore spin densities, to the Ga, In and Al nuclei in all of the complexes (**1**–**10**) were less than 0.5% (e.g., 0.3% for Al, 0.03–0.49% for Ga and 0.36% for In). The magnitude of the ^{69,71}Ga couplings also indicates that the unpaired electron spin density on the gallium nuclei in **4** and **6** remains very small (0.37% since $a_o=4356$ G for ^{69}Ga and $a_o=5535$ G for ^{71}Ga),[21] with only a negligible interaction to the iodine nucleus in **6** (0.4 G where $a_o=14844$ G for ^{127}I).

Complexes **5** and **6** have similar structures, with the only differences being the nature of the halogen ligand which presumably gives rise to the significantly different Ga–Ga bond lengths of 2.4662(12) Å for **5** and 2.5755(16) Å for **6**.

Table 1. Isotropic g and hyperfine coupling constants for complexes **1**–**10** derived by computer simulations of the room temperature X-band EPR spectra.

Complex[a]	g_{iso}	M[b]	^{1}H	^{14}N	X[c]	Ref
[(Ar-DAB$^{\cdot}$)AlI$_2$] (**1**)	2.0038	^{27}Al = 2.85	5.95	6.75	^{127}I = 0.38	[11]
[(Ar-DAB$^{\cdot}$)GaI$_2$] (**2**)	2.0036	^{69}Ga & ^{71}Ga ~25	~5.0	~5.0	^{127}I unresol	this work
[(*t*Bu-DAB$^{\cdot}$)GaI$_2$] (**3**)	2.0038	^{69}Ga = 1.3 ^{71}Ga = 1.65	1.4	8.62	^{127}I = 1.3	[11]
[(Ar-DAB)$_2$Ga] (**4**)	2.0032	^{69}Ga = 17.0 ^{71}Ga = 20.5	5.80	6.00	–	this work
[{(Ar-DAB$^{\cdot}$)GaBr}$_2$] (**5**)	2.0034	^{69}Ga = 22.5 ^{71}Ga = 27	5.8	6.0	^{79,81}Br = ~1.5	this work
[{(Ar-DAB$^{\cdot}$)GaI}$_2$] (**6**)	2.0032	^{69}Ga = 17.0 ^{71}Ga = 20.5	5.8	6.0	^{127}I = 0.4	this work
[{(*t*Bu-DAB$^{\cdot}$)GaI}$_2$] (**7**)	2.00385	^{69}Ga = 1.20 ^{71}Ga = 1.55	1.40	8.4	^{127}I = 1.30	[11]
[(Ar-DAB$^{\cdot}$)InCl$_2$(thf)] (**8**)	2.0012	^{115}In = 26.1 ^{113}In = 26.1	5	5	^{35,37}Cl = unresol.	this work
[{(Ar-DAB$^{\cdot}$)InCl}$_2$] (**9**)	2.0012	^{115}In = 26.2 ^{113}In = 26.1	5	5	^{35,37}Cl = unresol.	[10]
[(Ar-BIAN$^{\cdot}$)GaI$_2$] (**10**)	2.0063	^{69}Ga = 1.7 ^{71}Ga = 2.0	–	5.5	$2\times{}^{1}$H = 3.8	[14]

[a] Ar = 2,6-diisopropylphenyl. [b] M = Al, Ga or In. [c] X = ^{127}I, ^{35,37}Cl or ^{79,81}Br. All hyperfine values are given in Gauss (10 Gauss = 1 mT).

However, their corresponding EPR spectra, although different in profile, are not significantly different with respect to their diazabutadiene HFCs (Table 1), but have slight differences in their Ga and halogen HFCs which are presumably due to the different electronegatavities of the halogen ligands rather than different Ga–Ga bond lengths. The EPR spectrum of **5** (Figure 7) is ~120 G wide compared to 105 G

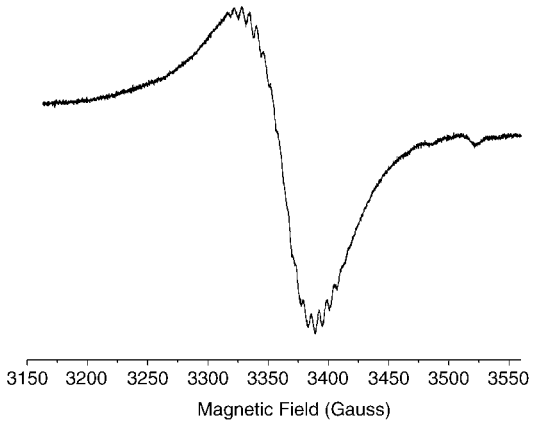

Figure 7. X-band EPR spectrum of **5** recorded at 298 K in 1:1 CD_2Cl_2/$C_6D_5CD_3$.

for **6**. The simulated spectrum of **5** (not shown) revealed a larger ^{69,71}Ga and halide HFC than that for **6**. This observation may be explained by the slightly greater electronegativity of bromine compared to iodine, which polarises the unpaired spin, creating a slightly larger delocalisation onto the gallium (0.49% in **5** compared to 0.36% in **6**) and bromine nuclei (a_{Br} ~1.5 G where a_o = 11443 G for ^{79}Br and a_o = 12335 G for ^{81}Br). Since the EPR spectra of **5** and **6** do not suggest an $S = 1$ electron–electron interacting system, the shorter Ga–Ga bond length in **5** should not influence the HFCs.

Unlike the well-resolved spectra of **4** and **6**, the room-temperature EPR spectrum of **2** produced a broad unresolved spectrum with a surprisingly larger spectral width of about 180 G (see Figure S2 in the Supporting Information). By comparison, the widths of the EPR spectra for the other gallium complexes substituted with aryl groups (**4**, **5** and **6**) were between about 105 and 120 G. Pott et al. recently reported the EPR spectrum for **2**, and interestingly their EPR spectrum was also broad and unresolved.[12] Hyperfine couplings of a_{Ga} = 27 G, a_N = 7 G and a_I = 8 G were estimated from the overall width of their spectrum. Surprisingly, however, no HFCs were reported for the two imine protons in that complex. Owing to the similarly poor resolution in our EPR spectrum of **2**, we also could only estimate the magnitude of the hyperfine couplings. A large ^{69,71}Ga interaction (of about ~25G) clearly contributes significantly to the overall width of the spectrum (this is particularly noticeable in the low-temperature spectrum shown later in the ENDOR section). However, the smaller ^{1}H, ^{14}N and ^{127}I couplings are difficult to estimate reliably without recourse to accurate simulations. The large ^{127}I HFC of 8 G reported by Pott et al.[12] was explained as originating from a hyperconjugative interaction of the gallium-iodine bonds with the π system of the Ar-DAB unit. However, in all of our studies of diazabutadiene complexes with Ga–I, Ga–Cl or Ga–Br fragments, only relatively small couplings to these Group 17 nuclei were systematically found (i.e., producing either unresolved hyperfine splittings or HFCs of less than 1.5 G). Furthermore, in a related study on the gallium(III)-pnictido complexes, [(*t*Bu-DAB$^{\cdot}$)Ga{E(SiMe$_3$)$_2$}$_n$I$_{2-n}$] (E = N, P or As; n = 1 or 2), negligible couplings to the electronegative N, P and As nuclei were also systematically observed by us.[13] Moreover, no direct evidence was found for such a large ^{127}I coupling of 8 G, as reported by Pott et al. in the ENDOR spectrum of **2** (as discussed later). Therefore, we believe that the estimated hyperfine values in Table 1 represent a better approximation to the HFCs of complex **2**.

While the unpaired electron density in all of the complexes studied (**1**–**9**) remains largely on the N_2C_2 diazabutadiene backbone, the subtle influence of the 1,4-N-substituents on the degree of delocalisation of the unpaired electron in the radical can be clearly seen in their EPR spectra. As discussed above, the ^{1}H and ^{14}N couplings are influenced by the presence of *tert*-butyl or aryl groups. However, these groups also appear to influence the spin density on the galli-

um nuclei where the complexes differ only in the presence of *t*butyl or aryl groups (for example 0.03% Ga spin density in **3** compared to about 0.49% in **2**). In addition, the overall spectral width in **2**, **4** and **6** decreases from 180 G (for **2**) to 105 G (for **4** and **6**), suggesting that the second ^{127}I nucleus in **2** (not visible in the EPR spectra) also makes a significant difference to the electron delocalisation in the radical and is largely responsible for the slightly greater polarisation of the unpaired electron spin away from the Ar-DAB ligand and onto the gallium nucleus (i.e., 0.49% Ga spin density on **2** compared to 0.36% on **4** and **6**).

The EPR spectrum and computer simulation of complex **8** is shown in Figure 8. The spectrum of the related dimeric

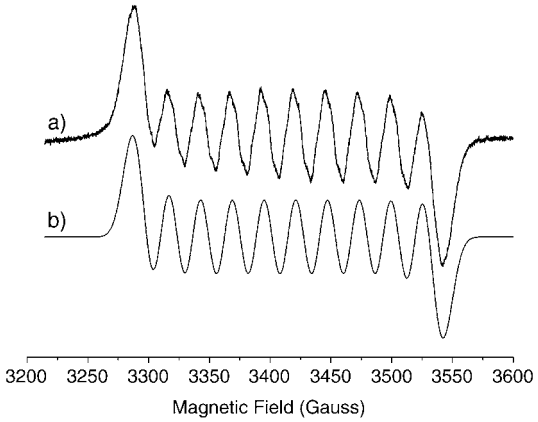

Figure 8. X-band EPR spectrum of **8** recorded at 298 K in 1:1 CD_2Cl_2/$C_6D_5CD_3$. a) experimental, b) simulated.

complex **9** was previously reported by us[10] and it was found that an identical set of spin Hamiltonian parameters could satisfactorily reproduce the spectra for both complexes. The isotropic couplings of 26.2 G for ^{115}In and 26.1 G for ^{113}In represent a 0.36% spin density on the In nuclei, similar to the values reported above for the gallium complexes, and confirming that the unpaired spin density remains largely on the Ar-DAB ligand in **8**. While the ^{113}In isotopic abundance is very small (4.3%), a satisfactory fit to the simulated line shape could not be achieved without this small contribution. It is interesting that similar hyperfine couplings were observed in both **8** and **9**, which suggests that the second Cl substituent, and indeed the oxidation state of the metal centre, do not alter the unpaired spin distribution in the indium complexes to any significant extent. This contrasts with the observations for the gallium complexes, **2** and **6**, where the second iodine creates a substantially different HFC to the gallium nucleus.

In all the gallium complexes containing two singly reduced DAB ligands (**5**, **6** and **7**; Scheme 1), no evidence was found for the presence of any dipole–dipole electron coupled systems at any temperature, as these would produce characteristic triplet states. In contrast, triplet state EPR spectra of the biradical systems [(*t*Bu-DAB)$_2$M] (M = Mg or Zn) were observed at 120 K by Gardiner et al.[8] In those cases, the distorted tetrahedral metal centres were directly chelated by two *t*Bu-DAB ligands, allowing dipole–dipole coupled interactions between the electrons. Such an interaction is clearly prohibited or substantially diminished by the intervention of the Ga–Ga bonds in **5**, **6** and **7**, thus producing a doublet ground state in each of these complexes.

The EPR spectrum of **10** is shown in Figure 9. The spectrum was simulated using HFCs of $a_{69Ga} = 1.7$ G, $a_{71Ga} = 2.0$ G, $a_N = 5.5$ G and $a_H = 3.8$ G for two magnetically equiva-

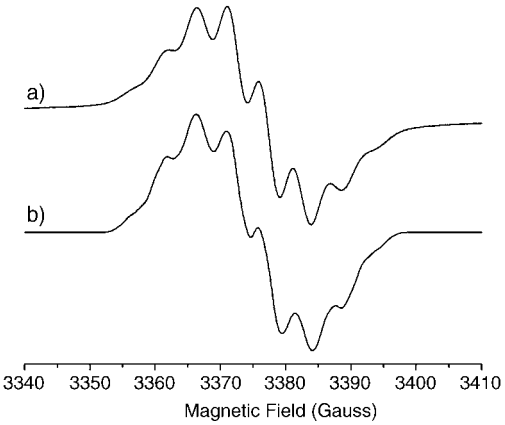

Figure 9. X-band EPR spectrum of **10** recorded at 298 K in 1:1 CD_2Cl_2/$C_6D_5CD_3$. a) experimental, b) simulated.

lent ^{14}N and ^{1}H nuclei. Unlike all of the previous complexes (**1**–**9**), the two imine protons are absent in complex **10** due to the naphthalene backbone of its diimine ligand. Considering that imine proton couplings of about 5.5 G are normally observed for the aryl-substituted diazabutadiene ligands (Table 1), the observed 3.8 G coupling in **10** (with no imine protons) is significant and must be assigned to the ring protons (labelled H^1 in Scheme 1) of the naphthalene fragment. Recently Fedushkin et al.,[22] reported the EPR spectra of the mono- and trianions of the same 1,2-bis{(2,6-diisopropylphenyl)imino}acenaphthene ligand (Ar-BIAN) in complexes with alkali metal cations. The dimeric sodium derivative of the monoanion (ie., $[Na^+(Ar\text{-}BIAN)^-]_2$) produced resolved couplings to two nitrogen nuclei (4.6 G) and two sodium nuclei (1.7 G), indicating that the unpaired electron was mainly localised over the diimine part of the Ar-BIAN ligand. However, no couplings were observed to the nitrogen atoms in the trianion, $[Na^+_3(Et_2O)_2(Ar\text{-}BIAN)^{3-}]$, and instead the EPR spectrum displayed couplings to three different pairs of ^{1}H nuclei (ie., $a_H = 0.27$ G, $a_H = 3.9$ G and $a_H = 6.6$ G), indicating spin delocalisation over the naphthalene part of the ligand. The 3.8 G HFC observed in **10**, must therefore arise from spin delocalisation away from the diimine fragment and into the naphthalene part of the Ar-BIAN ligand, thus producing a HFC constant analogous to that found in the Ar-BIAN trianion case. Hyperfine couplings to the remaining two sets of protons (H^2 and H^3,

Scheme 1) could not be resolved by EPR, but were detected in the ENDOR experiment (discussed later).

As unpaired electron delocalisation occurs into the naphthalene fragment of **10**, the couplings to the nitrogen nuclei were slightly reduced to 5.5 G, relative to the situation in the related Ar-DAB complexes, **4**–**6**. Moreover, the gallium hyperfine couplings were dramatically reduced to only 1.7 G and 2.0 G for ^{69}Ga and ^{71}Ga, respectively, which represents an approximately 0.05% isotropic spin density on the gallium nucleus in **10** compared to about 0.37% in **2**, **4** and **6**. Since the extent of spin delocalisation onto ^{69,71}Ga is so small in **10**, it is not surprising that the ^{127}I interactions could not be observed in the EPR spectrum.

ENDOR investigations: Owing to the higher resolving power of the electron nuclear double resonance (ENDOR) technique, a significant enhancement in spectral resolution can be obtained compared to the EPR technique, particularly for π based organic radicals. In many of the above complexes, minimum line widths of 3–5 G (8–14 MHz) were observed. In ENDOR spectroscopy line widths of only 0.3 MHz are commonly observed, so hyperfine interactions that are masked by the width of the EPR line can be resolved. Therefore, while the fluid solution EPR spectra revealed the larger HFCs to ^{69,71}Ga, ^{14}N and imine-^{1}H nuclei of the diimine ligands in **1**–**10**, cw ENDOR can be used to detect the much weaker hyperfine couplings to the more remote protons of the *tert*-butyl or aryl groups. In this way, a more precise description of the extent of the spin delocalisation in the paramagnetic compounds can be obtained. We were unable to obtain the fluid solution cw ENDOR spectra of the radicals in the chosen solvents, so the low-temperature (10 K) frozen solution ENDOR spectra were obtained and revealed the added contributions from the anisotropic hyperfine interactions.

For an $S=1/2$ ground state organic radical in an isotropic solution interacting with a single proton, two ENDOR lines are expected at the resonance frequencies $\nu_{ENDOR}=|\nu_n \pm {}^1/_2 a_{iso}|$, where ν_n is the nuclear Larmor frequency and a_{iso} (or a) the isotropic hyperfine coupling (HFC). If, however, ν_n is less than ${}^1/_2 a$ then two lines are expected, separated by $2\nu_n$ and centred on $a/2$. In frozen solution, a more complex powder type ENDOR pattern is observed, due to absorptions from a range of orientations of the radical with respect to the direction of the magnetic field, and many more lines can be obtained. As a result, the ENDOR lines broaden and may become very weak unless the coupling is dominated by a particular dipolar interaction. Reasonably narrow lines can be observed in powder ENDOR spectra only if the hyperfine anisotropy pertaining to the nucleus is small. For π-based organic radicals, readily observable coupling constants generally arise from α and β protons. For α protons the anisotropy typically amounts to about 50% of the magnitude of the isotropic hyperfine coupling a and the principal hyperfine tensor values are roughly $1/2a$, a and $3/2a$. The anisotropy of the β protons is typically much smaller at about 20%.[24]

In both of the *tert*-butyl substituted complexes (**3** and **7**), relatively small HFCs of 1.4 G (3.92 MHz) were observed by EPR for the imine protons (see Table 1). A more accurate measure of this coupling can be obtained by ENDOR, and pairs of lines should therefore be observed centred on ν_n for the protons which should be separated by approximately 1.96, 3.92 and 5.88 MHz. In fact, α-proton couplings (arising from the two imine protons of the diazabutadiene ligand) of a similar magnitude were observed by us in the low-temperature ENDOR spectra of a related series of pnictidogallium(III) diazabutadiene complexes.[13] The frozen solution (10 K) ENDOR spectra of **3** and **7** are shown in Figure 10a and b, respectively. Both spectra are virtually identical, indicating a similar degree of unpaired electron interaction with the remote protons in both complexes. Only the imine proton couplings corresponding to a (3.4 MHz) and ${}^1/_2 a$ (1.68 MHz) could be resolved in each spectrum, since the $3/2a$ coupling was too broad to be clearly detected even at high RF modulation. Assuming a negative sign for the isotropic coupling of the α protons,[23] the a_{iso} value estimated by ENDOR for **3** and **7** is 3.39 MHz

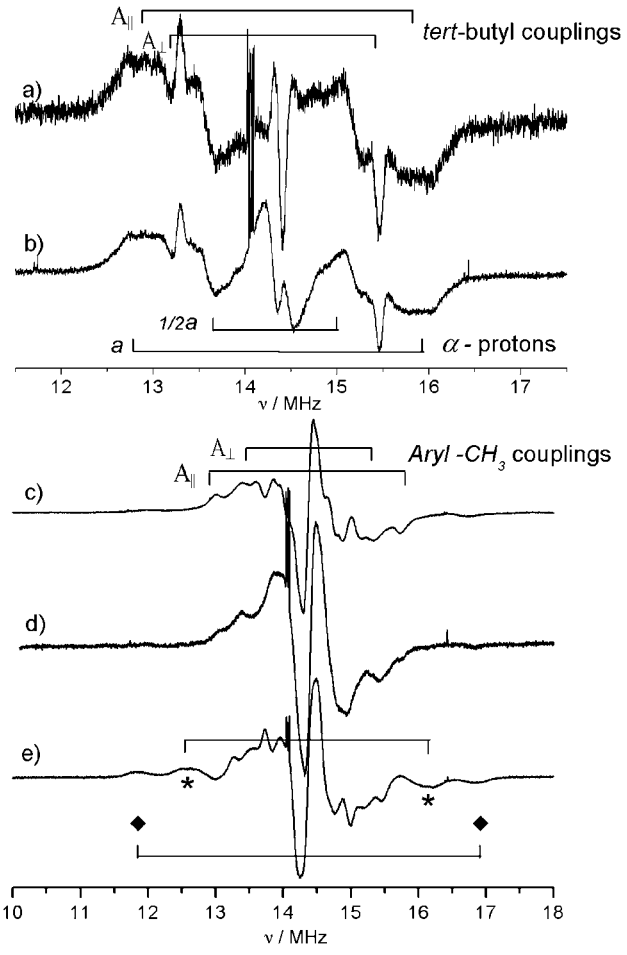

Figure 10. X-band cw ENDOR spectra (10 K) of the *tert*-butyl substituted complexes a) **3** and b) **7**, and the aryl-substituted complexes c) **4**, d) **6** and e) **10.**

(1.21 G), which is similar to the value derived by EPR spectroscopy (1.4 G) from the room-temperature spectra.

The remaining peaks in the ^{1}H ENDOR spectra of **3** and **7** arise from couplings to their bulky *tert*-butyl group protons. The principal components of the anisotropic hyperfine tensors for methyl group protons should be visible in the powder ENDOR spectra. The three protons of the freely rotating methyl groups are equivalent on the EPR timescale, producing an axial hyperfine tensor, and the hyperfine anisotropy is usually less than 20% of a_{iso}. A build up of intensity in the ENDOR spectrum is expected at about $0.95a$ and $1.1a$, close to the isotropic coupling. The resonances found at $A_{\parallel}=2.7$ MHz and $A_{\perp}=2.16$ MHz in Figure 10a,b (i.e., $1.1a$ and $0.95a$) can therefore be assigned to the interactions of the unpaired electron with the protons of closer methyl groups of the *tert*-butyl substituents. The intense inner line in Figure 10a, which is centred exactly on ν_n, likely arises from a matrix ENDOR line originating from purely dipolar interactions to remote nuclei. However, two pairs of poorly resolved lines can be clearly observed in Figure 10b, with a coupling of about 0.3 MHz, which can be tentatively assigned to weak couplings from the protons of the more remote methyl groups of the *tert*-butyl substituents.

The ^{1}H ENDOR spectra of the aryl-substituted complexes **4**, **6** and **10** are shown in Figure 10c, d and e respectively. The spectra of **4** and **6** are very similar to each other, while the spectrum of **10** contains additional peaks arising from the protons of the acenaphthene group (labelled H^2 and H^3 in Scheme 1). These powder ENDOR spectra primarily arise from weak hyperfine couplings to the ring protons (H^4 and H^5) and methyl protons (H^6) of the aryl groups with a small contribution from the methine proton. According to the EPR spectra, the α-proton couplings from the Ar-DAB ligand were 5.5 G (16.2 MHz). This produces very broad resonances that could not be easily detected in the cw ENDOR spectrum, even at high RF modulation amplitudes. Couplings to the protons of the methyl groups (labelled H^6) were observed at $A_{\parallel}=2.72$ MHz and $A_{\perp}=1.95$ MHz for **4**, $A_{\parallel}=2.66$ MHz and $A_{\perp}=2.02$ MHz for **6** and $A_{\parallel}=2.16$ MHz and $A_{\perp}=1.68$ MHz for **10**. The slight differences in these couplings are likely related to small differences in the steric environment or twist angle of the aryl groups in each respective complex. Since this coupling is largely dipolar, small changes in the spatial orientation of the methyl groups will indirectly influence the magnitude of the coupling. The remaining peaks in the ^{1}H ENDOR spectra of **4** and **6** can be assigned to the aryl ring protons (H^4 or H^5 in Scheme 1). The hyperfine couplings to these ring protons are relatively large considering their distance from the gallium heterocycles in each complex. The peaks separated by 4.79, 4.84 and 5.04 MHz in the ENDOR spectra of **4**, **6** and **10** respectively (labelled ◆ in Figure 10e for example) are due to a single component of the H^4 or H^5 hyperfine tensor, whereas the other components (expected to be smaller) are buried within the powder pattern and are difficult to extract. It can, however, be proposed that the inner peaks separated by about 1.07 MHz and about 0.6 MHz in the ENDOR spectra, are due to the remaining components of this hyperfine tensor.

Two additional peaks can also be detected in the ENDOR spectra of **10** (labelled * in Figure 10e), separated by 3.728 and 3.278 MHz, which are clearly absent in the ENDOR spectra of **4** and **6**. These couplings can be assigned to the *meta* or *para* protons (H^2 or H^3) of the acenaphthene ring (the H^1 *ortho*-protons produced a 10.36 MHz coupling; Table 1) and their magnitude is likely due to spin delocalisation into these rings arising from a hyperconjugation mechanism. The other components of the hyperfine tensor cannot be resolved, so the 3.728 and 3.278 MHz couplings likely represent the largest couplings in the tensor.

The ENDOR spectra for the aryl-substituted mono-gallium complex **2** are shown in Figure 11. Owing to the small g anisotropy in the EPR spectrum, very little angular selection is expected in the ENDOR spectra recorded at different field positions. However, due to the relatively large gallium

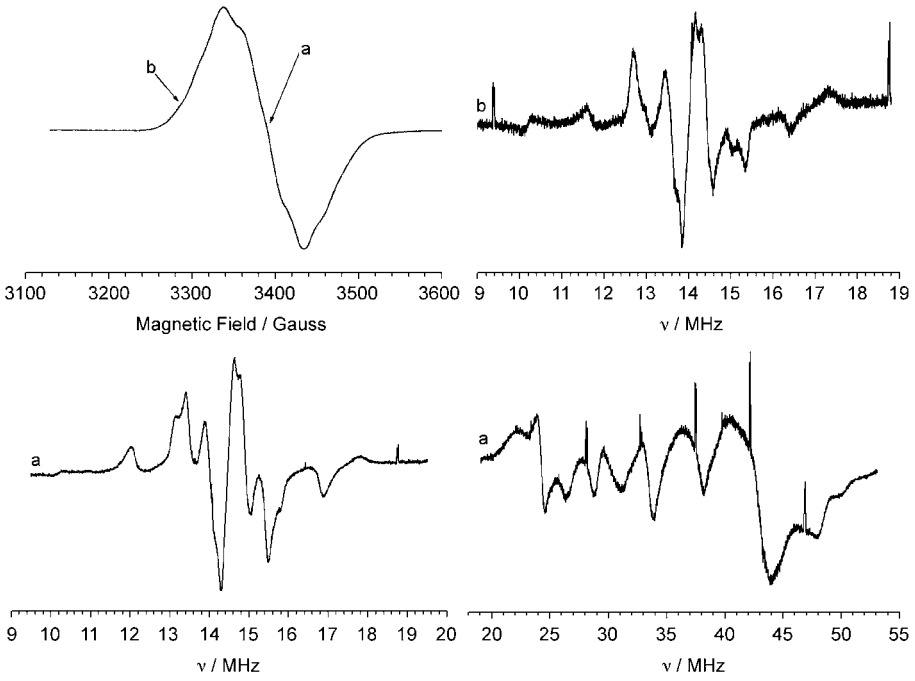

Figure 11. X-band EPR and ENDOR spectra of **2** recorded at 10 K in 1:1 $CD_2Cl_2/C_6D_5CD_3$. The field positions for the ENDOR measurements are labelled (a) and (b).

hyperfine couplings, small variations may be expected in the ENDOR spectra arising from anisotropy in the gallium coupling. The peaks separated by 2.65 MHz and 2.088 MHz can be easily assigned to the parallel and perpendicular components of the aryl methyl protons. The remaining peaks, dominated by the large coupling at 4.88 MHz, can again be assigned to the largest component of the hyperfine tensor for the aryl-ring protons, similar to that observed in the spectra of **4**, **6** and **10**. However, the most unique features in the ENDOR spectrum of **2** are the strong resonances in the region of 20 MHz to 55 MHz. These peaks were not observed in any of the other compounds. It should be recalled that the EPR features of this particular sample were also unusual, producing a broad unresolved spectrum with a substantially large spectral width (of ~180 G) compared to those of the other complexes. These unusual EPR features appear to be accompanied by unusual ENDOR features (i.e., the appearance of new resonances from 20–55 MHz) which we assign to ^{69,71}Ga couplings. While gallium ENDOR signals have been widely reported in doped semiconductor systems,[25] this is to the best of our knowledge the first observation of gallium ENDOR signals in any discrete molecular metal complex system.

The interpretation of the gallium ENDOR signals in Figure 11 is complicated by a number of factors, including: 1) the powder type ENDOR pattern which will potentially produce overlapping signals from the anisotropic hyperfine (A) and quadrupolar (Q) tensors, 2) the different nuclear Larmor frequencies (ν_n) of the two isotopes (3.5867 MHz for ^{69}Ga and 4.6913 MHz for ^{71}Ga at 3500G), 3) the different and substantial electric quadrupolar moments of these $I=$ 3/2 nuclei (0.168×10^{24} cm^2 for ^{69}Ga and 0.106×10^{24} cm^2 for ^{71}Ga), and 4) the different isotopic abundances of the nuclei. Because the isotropic HFC estimated from the EPR spectrum was about 25 G, and therefore larger than ν_n, the ENDOR peaks will be centred on $a/2$ and separated by $2\nu_n$. For $I>1$ spin systems ENDOR peaks are expected at the resonant frequencies of $\nu_{ENDOR} = |A_i/2 \pm \nu_n \pm 3/2Q_i\ (2\,m_I + 1)|$, so that each ENDOR line will be further split into $2I$ equidistant lines spaced by the quadrupole splittings. A preliminary simulation and analysis of this spectrum suggests that the hyperfine tensors are $A=$ (67, 74, 86) MHz, while the quadrupolar couplings are less that 0.1 MHz.

The ENDOR spectra of the mononuclear aluminium complex, **1**, and the dimeric indium complex, **9**, are shown in Figure 12a and b. The low-temperature EPR spectra and the ^{1}H ENDOR spectra measured at different field positions for **1** and **9** are shown in the Supporting Information. Despite the differences in the metal coordination environments for **1**, **9** and the series of aryl substituted gallium complexes, the ^{1}H ENDOR spectra of all complexes remain very similar. As discussed above for **4**, **6** and **10**, the largest coupling to the H^4 or H^5 aromatic protons of the aryl group protons can be clearly seen in the spectra of **1** and **9** (4.91 MHz and 4.90 MHz for **1** and **9** respectively). Couplings to the methyl protons (H^6) of the aryl groups can also be observed ($A_\parallel=$ 2.55 MHz and $A_\perp=2.08$ MHz for **1** and $A_\parallel=2.50$ MHz and $A_\perp=2.28$ MHz for **9**) in addition to the poorly resolved inner peaks arising from the other components of the H^4 or H^5 tensor. These results clearly indicate that differences in the metal centres do not greatly influence the unpaired spin density on the aryl groups in any of the complexes.

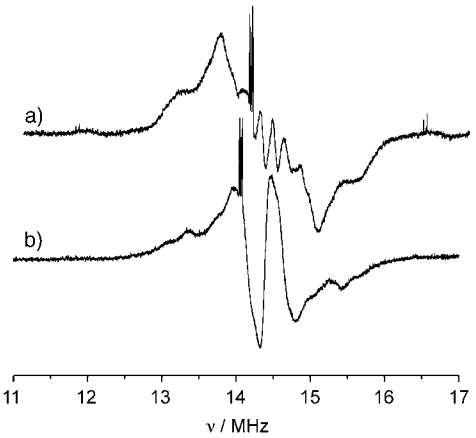

Figure 12. X-band cw ENDOR spectra (10 K) of the complexes: a) **1** and b) **9.**

Conclusion

In summary, a number of novel paramagnetic heterocyclic compounds containing $Ga^{II,III}$ or In^{III} centres have been prepared and structurally characterised. These compounds and a series of previously reported systems have been characterised by EPR and ENDOR spectroscopies, which provided detailed information on the structural and electronic properties of the radicals. These results have confirmed that the unpaired electron in all compounds is mainly centred on the diimine backbone, with relatively weak interactions to the coordinated Al, Ga and In nuclei. Changes in unpaired electron spin density were found to be markedly dependent on the nature of the bulky substituents at the 1,4 positions of the diimine ligands. In one compound, **2**, well resolved gallium hyperfine and quadrupolar couplings were detected for the first time, although it remains unclear why only one gallium complex revealed these gallium ENDOR couplings. Spin doublet ground states were present in all complexes, despite the close proximity of two singly reduced diazabutadiene ligands in the dimeric complexes (**5**, **6** , **7** and **9**), while no dynamic Jahn–Teller distortions due to electron transfer from one Ar-DAB ligand to the other were detected in [(Ar-DAB)$_2$Ga].

Experimental Section

All manipulations were carried out using standard Schlenk and glove box techniques under an atmosphere of high purity argon. Toluene, DME, THF and [D_8]toluene were distilled over potassium. Diethyl ether was distilled over Na/K, whilst CD_2Cl_2 was distilled over CaH_2 then freeze/

thaw degassed prior to use. The EPR/ENDOR spectra were recorded on a cw X-Band Bruker ESP300E series spectrometer equipped with an ESP360 DICE ENDOR unit, operating at 12.5 kHz field modulation in a Bruker EN801 cavity. ENDOR spectra were recorded at 10 K using an Oxford instruments ESR 900 continuous flow He Cryostat. The ENDOR spectra were obtained using 10 dB RF power from an ENI A-300 RF amplifier at 75 kHz or 200 kHz RF modulation depth. EPR computer simulations were carried out using the commercial Bruker's Simfonia program. Mass spectra were recorded using a VG Fisons Platform II instrument under APCI conditions. IR spectra were recorded using a Nicolet 510 FT-IR spectrometer as Nujol mulls between NaCl plates. Melting points were determined in sealed glass capillaries under argon, and are uncorrected. Reproducible microanalyses could not be obtained on new complexes due to inclusion of solvent of crystallisation and/or their air- and moisture-sensitive nature. The compounds [K(tmeda)][:Ga(Ar-DAB)],[11] "GaI",[26] Ar-DAB[27] and $[MoBr_2(CO)_2(PPh_3)_2]$[28] were prepared according to literature methods.

[(Ar-DAB)$_2$Ga] (4) and [{(Ar-DAB·)GaI}$_2$] (6): To a suspension of "GaI" (1.18 mmol) in toluene (20 mL) held at −78 °C was added a solution of [K(tmeda)][:Ga(Ar-DAB)] (0.71 g, 0.59 mmol) in toluene (15 mL). The mixture was warmed to room temperature and stirred overnight to give a red solution. The solvent was removed in vacuo and the residue extracted firstly with diethyl ether (20 mL) then with toluene (20 mL). Concentration of the diethyl ether extract and placement at −35 °C yielded red crystals of **6** overnight (0.08 g, 12 %). The toluene extract was also concentrated and placed at −35 °C to give red crystals of **4** overnight (0.12 g, 25 %). **4**: M.p. 176–179 °C (decomp); IR (Nujol): $\tilde{\nu}$ = 1381 (w), 1360 (m), 1314 (m), 1250 (s), 1227 (m), 1201 (m), 1110 (s), 933 (w), 800 (s), 758 (s), 656 cm^{-1} (w); MS (APCI): *m*/*z* (%): 377 (100) [Ar-DAB$^+$]; **6**: M.p. 161–164 °C (decomp); IR (Nujol): $\tilde{\nu}$ = 1661 (m), 1379 (m), 1361 (w), 1319 (m), 1259 (m), 1224 (m), 1098 (br), 797 (s), 753 cm^{-1} (m); MS (APCI): *m*/*z* (%): 573 (10) [(Ar-DAB)GaI$^+$], 377 (100), [Ar-DAB$^+$].

[{(Ar-DAB·)GaBr}$_2$] (5): To a solution of $[MoBr_2(CO)_2(PPh_3)_2]$ (0.69 g, 0.82 mmol) in Et_2O (10 mL)/DME (5 mL) held at −78 °C was added a solution of [K(tmeda)][:Ga(Ar-DAB)] (0.50 g, 0.42 mmol) in Et_2O (15 mL). The mixture was warmed to room temperature and stirred for 3 h to give a red solution. The solvent was removed in vacuo and the residue extracted with DME (20 mL). Concentration and placement at −35 °C yielded red crystals of **5** (0.16 g, 36 %). M.p. 152–154 °C (decomp); IR (Nujol): $\tilde{\nu}$ = 1381 (m), 1361 (m), 1320 (m), 1258 (m), 1226 (m), 1097 (s), 1051 (w), 937 (m), 797 (m), 754 (m), 695 cm^{-1} (w); MS (APCI): *m*/*z* (%): 377 (100) [Ar-DAB$^+$].

[(Ar-DAB·)InCl$_2$(thf)] (8): To a solution of Ar-DAB (0.5 g, 1.33 mmol) in Et_2O/THF (10 mL/5 mL) was added a suspension of Li powder (0.1 g, 14.0 mmol) in Et_2O (15 mL) at −78 °C. The suspension was warmed up to room temperature and stirred for 3 hrs to yield an orange solution. Filtration yielded a clear, red solution of [(Ar-DAB)Li$_2$]. A suspension of InCl (0.40 g, 2.66 mmol) in Et_2O (15 mL) was then added at −78 °C. The resulting solution was warmed to room temperature and stirred overnight to give a red solution and a precipitate of indium metal. The reaction mixture was filtered, volatiles removed in vacuo and the residue extracted into Et_2O (10 cm^3). Cooling the extract to −30 °C yielded red crystals of **8** (0.02 g, < 5 %); m.p, 142–144 °C (decomp); IR (Nujol): $\tilde{\nu}$ = 1625 (s), 1260 (s), 1098 (s), 800 (s), 760 cm^{-1} (s); MS (APCI): *m*/*z* (%): 377 (100) [Ar-DAB$^+$].

X-ray crystallography: Crystals of **4, 5, 6**, and **8** suitable for X-ray structural determination were mounted in silicone oil. Crystallographic measurements were made using a Nonius Kappa CCD diffractometer. The structures were solved by direct methods and refined on F^2 by full-matrix least-squares (SHELX97)[29] using all unique data. All non-hydrogen atoms are anisotropic with H-atoms included in calculated positions (riding model). Crystal data, details of data collections and refinement are given in Table 2.

CCDC-253980 (**4**), CCDC-253981 (**5**), CCDC-253982 (**6**) and CCDC-253983 (**8**) contain the supplementary crystallographic data for this paper. These data can be obtained free of charge from The Cambridge Crystallographic Data Centre via www.ccdc.cam.ac.uk/data request/cif.

Table 2. Crystal data for complexes **4**, **5**, **6** and **8**.

	4	**5**·(DME)$_2$	**6**·(Et$_2$O)$_2$	**8**
chemical formula	$C_{52}H_{72}GaN_4$	$C_{60}H_{92}Br_2Ga_2N_2O_4$	$C_{60}H_{92}Ga_2I_2N_4O_2$	$C_{30}H_{44}Cl_2InN_2O$
FW	822.86	1232.64	1294.62	634.39
crystal system	monoclinic	triclinic	triclinic	triclinic
space group	*C*2/*c*	$P\bar{1}$	$P\bar{1}$	$P\bar{1}$
a [Å]	24.640(5)	9.6880(19)	9.7190(19)	13.123(3)
b [Å]	9.0420(18)	12.839(3)	12.799(3)	13.434(3)
c [Å]	23.038(5)	14.130(3)	14.141(3)	18.102(4)
α [°]	90	94.47(3)	94.37(3)	97.96(3)
β [°]	114.26(3)	105.56(3)	105.67(3)	90.32(3)
γ [°]	90	111.86(3)	110.91(3)	91.40(3)
V [Å^3]	4679.5(16)	1540.0(5)	1552.7(5)	3159.5(11)
Z	4	4	1	4
T [K]	150(2)	150(2)	150(2)	150(2)
$\mu(Mo_{K\alpha})$ [mm^{-1}]	0.626	2.218	1.903	0.941
reflections collected	38433	25286	25543	58483
unique reflections [R_{int}]	5345 (0.0901)	6970 (0.0977)	7043 (0.0557)	14399 (0.0876)
*R*1 ($I > 2\sigma(I)$)	0.0461	0.0508	0.0558	0.0639
*wR*2 (all data)	0.1053	0.1057	0.1247	0.1659

Acknowledgements

We thank the EPSRC (partial studentship for M.K. and postdoctoral fellowship for R.J.B.) and Nuffield foundation (D.P.M., Grant No. NUFURB03) for financial support. The EPSRC National Service for Electron Paramagnetic Resonance (GR/R17980/01) is also thanked.

[1] P. P. Power, *Chem. Rev.* **2003**, *103*, 789–809.
[2] W. J. Kaim, *J. Organomet. Chem.* **1981**, *215*, 325–335.
[3] J. Braddock-Wilking, J. T. Leman, C. T. Farrar, S. C. Larsen, D. J. Singel, A. R. Barron, *J. Am. Chem. Soc.* **1995**, *117*, 1736–1745.
[4] F. G. N. Cloke, C. I. Dalby, M. J. Henderson, P. B. Hitchcock, C. H. L. Kennard, R. N. Lamb, C. L. Raston, *J. Chem. Soc. Chem. Commun.* **1990**, 1394–1396.
[5] F. G. N. Cloke, G. R. Hanson, M. J. Henderson, P. B. Hitchcock, C. L. Raston, *J. Chem. Soc. Chem. Commun.* **1989**, 1002–1003.
[6] W. Kaim, W. Matheis, *J. Chem. Soc. Chem. Commun.* **1991**, 597–598.
[7] F. G. N. Cloke, C. I. Dalby, P. J. Daff, J. C. Green, *J. Chem. Soc. Dalton Trans.* **1991**, 181–184.
[8] M. C. Gardiner, G. R. Hanson, M. J. Henderson, F. C. Lee, C. L. Raston, *Inorg. Chem.* **1994**, *33*, 2456–2461.
[9] P. Clopath, A. von Zelewsky, *Helv. Chim. Acta* **1973**, *56*, 980–983.
[10] R. J. Baker, R. D. Farley, C. Jones, M. Kloth, D. M. Murphy, *Chem. Commun.* **2002**, 1196–1197.
[11] R. J. Baker, R. D. Farley, C. Jones, M. Kloth, D. M. Murphy, *J. Chem. Soc. Dalton Trans.* **2002**, 3844–3850.

[12] T. Pott, P. Jutzi, W. Kaim, W. W. Schoeller, B. Neumann, A. Stammler, H.-G. Stammler, M. Wanner, *Organometallics* **2002**, *21*, 3169–3172.
[13] K. A. Antcliff, R. J. Baker, C. Jones, D. M. Murphy, R. P. Rose, *Inorg. Chem.* **2005**, in press.
[14] R. J. Baker, C. Jones, M. Kloth, D. P. Mills, *New J. Chem.* **2004**, *28*, 207–213.
[15] a) E. S. Schmidt, A. Jockisch, H. Schmidbaur, *J. Am. Chem. Soc.* **1999**, *121*, 9758–9759; b) E. S. Schmidt, A. Schier, H. Schmidbaur, *J. Chem. Soc. Dalton Trans.* **2001**, 505–507.
[16] R. J. Baker, C. Jones, M. Kloth, J. A. Platts, *Angew. Chem.* **2003**, *115*, 2764–2767; R. J. Baker, C. Jones, M. Kloth, J. A. Platts, *Angew. Chem.* **2003**, *115*, 2764–2767; *Angew. Chem. Int. Ed.* **2003**, *42*, 2660–2663.
[17] a) R. J. Baker, C. Jones, J. A. Platts, *J. Am. Chem. Soc.* **2003**, *125*, 10534–10535; b) R. J. Baker, C. Jones, J. A. Platts, *Dalton Trans.* **2003**, 3673–3674.
[18] T. Steinke, C. Gemel, M. Cokoja, M. Winter, R. A. Fischer, *Chem. Commun.* **2003**, 1066–1067, and references therein.
[19] R. J. Baker, A. J. Davies, C. Jones, M. Kloth, *J. Organomet. Chem.* **2002**, *656*, 203–210.
[20] W. W. Schoeller, S. Grigoleit, *J. Chem. Soc. Dalton Trans.* **2002**, 405–409.
[21] J. A. Weil, J. R. Bolton, J. E. Wertz, *Electron Paramagnetic Resonance*, Wiley, **1994**, p. 534.
[22] I. L. Fedushkin, A. A. Skatova, V. A. Chudakova, V. K. Cherkasov, G. K. Fukin, M. A. Lopatin, *Eur. J. Inorg. Chem.* **2004**, 388–393.
[23] H. Kurreck, B. Kirste, W. Lubitz, *Electron Nuclear Double Resonance Spectroscopy of Radicals in Solution*, VCH Publishers, **1988**.
[24] P. J. O'Malley, G. T. Babcock, *J. Am. Chem. Soc.* **1986**, *108*, 3995–4001.
[25] K. T. Stevens, N. Y. Garces, L. Bai, N. C. Giles, L. E. Halliburton, S. D. Setzler, P. G. Schunemann, T. M. Pollak, R. K. Route, R. S. Feigelson, *J. Phys. Condens. Matter* **2004**, *16*, 2593–2607.
[26] M. L. H. Green, P. Mountford, G. J. Smout, S. R. Peel, *Polyhedron* **1990**, *9*, 2763–2765.
[27] L. Jafarpour, E. D. Stevens, S. P. Nolan, *J. Organomet. Chem.* **2000**, *606*, 49–54.
[28] J. R. Backhoue, H. M. Lowe, E. Sinn, S. Suzuki, S. Woodward, *J. Chem. Soc. Dalton Trans.* **1995**, 1489–1496.
[29] G. M. Sheldrick, SHELX-97, Program for the Solution of Crystal Structures, University of Göttingen, Göttingen (Germany), **1997**.

Received: November 2, 2004
Published online: March 10, 2005